ELSEVIER

Weathering of the Ganga alluvial plain, northern India: implications from fluvial geochemistry of the Gomati River

Munendra Singh [a,*], Maneesh Sharma [b], Heinz Jürgen Tobschall [b]

[a] *Department of Geology, University of Lucknow, Lucknow 226 007, India*
[b] *Institute of Geology and Mineralogy, University of Erlangen-Nuremberg, D-91054 Erlangen, Germany*

Abstract

In the northern part of the Indian sub-continent, the Ganga alluvial plain (GAP) feeds its weathering products to the Ganga–Brahmaputra River system, one of the world's largest fluvial systems. The authors present a geochemical study of the GAP weathering products transported by the Gomati River (the Ganga River tributary) to understand weathering processes of an alluvial plain in a humid sub-tropical climate. A total of 28 sediment samples were collected during the monsoon season and were analysed by X-ray fluorescence spectrometry for 25 major and trace elements. Bulk chemistry of the channel, flood and suspended sediments mostly consists (>90%, >80% and >75%, respectively) of three elements; Al, Si and Fe. Major element concentrations normalised with respect to upper continental crust (UCC) show strong depletion of highly mobile elements (Na, Ca) and enrichment of immobile elements (Ti, Si). Silica enrichment in the sand fraction is probably caused by chemical weathering of feldspar. Mineral sorting during fluvial transportation acts as the single important factor that controls the geochemistry of these weathering products and also strongly influences major and trace element distribution in the individual sediment samples. Trace element (Ba, Cr, Cu, Nb, Ni, Pb, V and Zn) concentrations were strongly correlated with major element (Si, Al, Fe, Mn and K) concentrations indicating that the abundance of trace elements is controlled by the same processes that control the major element distribution in these sediments.

The GAP weathering products were geochemically distinguished as arkose to litharenite in rock classification. Chemical mobility, normalised with respect to TiO_2 in UCC, indicates that Si, Na, Zr, Ba and Sr, mainly derived from feldspar, muscovite and biotite, are lost during weathering. Iron and Zn remained immobile during weathering and were strongly adsorbed by phyllosilicates and concentrated in fine-grained sediment fractions. The chemical index of alteration indicates that the GAP has experienced chemical weathering of incipient to moderate intensity. The GAP weathering products also demonstrated a progressive incomplete alteration in the alluvial sequence made-up of the Himalayan-derived sediments. A model has been proposed to better understand weathering processes and products of the GAP in temporary storage of ~50 ka in a humid sub-tropical climate.

---

1. Introduction

* Corresponding author. Fax: +91 522 2740037.
E-mail address: smunendra@usa.net (M. Singh).

Continental physical and chemical weathering are the principal processes by which terrigenous clastic

materials are produced from continents, transported into oceans and modified prior to deposition. These weathering processes, therefore, are of considerable importance both in geological interpretation of sedimentary sequences and in understanding the effects of human modifications of the physical environmental system (Robinson and Johnsson, 1997; Huh et al., 1998). Their weathering products are a cumulative result of lithology, degree of physical and chemical weathering experienced by the source area and subsequent changes during transportation and deposition processes. Comprehensive geological studies of weathering processes and products are required to interpret sedimentary sequences in a better way and to investigate average crustal composition as a constraint on a model of large scale crustal evolution through geological time (McLennan et al., 1980; Taylor and McLennan, 1981; Bhatia, 1983; McLennan and Taylor, 1983; Wronkiewicz and Condie, 1987; Cullers, 1988; Nesbitt and Young, 1984, 1989; Garver and Scott, 1995; Fedo et al., 1996).

The most spectacular landscape formed during the post-continental collision between the Indian and Asian continents is the Indo-Ganga–Brahmaputra Plain, the world's largest alluvial tract. It separates the Himalayan orogenic belt from the Indian Craton. The middle part of the Indo-Ganga–Brahmaputra Plain is known as the Ganga Plain. Asian rivers are the chief transporting agent of continental weathering products and supply as much as 30% of the global sediment input to the world's ocean (Milliman and Meade, 1983). Weathering products of the Ganga Plain are transported downstream by the Ganga River system and subsequently get deposited either in the Ganga Delta or in the Bengal Deep-Sea Fan regions (Fig. 1). The Gomati River basin that drains a part of the Ganga Plain provides the most prominent site to understand weathering processes and products of the GAP. Major rivers of the world have been investigated by several geochemists for their continental weathering materials (Potter, 1978, 1994; Dupré et al., 1996; Canfield, 1997; Vital and Stattegger, 2000). Sarin et al. (1989) studied major ion chemistry of the Ganga–Brahmaputra river system to understand weathering processes of the region and elemental fluxes of the rivers to the Bay of Bengal. Several studies have been done to understand the geological evolution, fluvial processes, sedimentology and environmental problems in the GAP (Abbas and Subramaniam, 1984; Ajmal et al., 1985; Subramaniam et al., 1987a,b; Kumar, 1989; Faruqui et al., 1992; Singh et al., 1997; Ansari et al., 1998, 2001). In contrast to this, weathering studies of the GAP have received a little attention so far.

The present investigation was undertaken to obtain a better understanding of the GAP weathering processes and to explore the implication of weathering of an alluvium sequence in temporary storage of ~50 ka under a humid sub-tropical climate. The aims of this reconnaissance study were to gain complementary insight into: (i) major and trace element distribution in the GAP weathering products; (ii) the nature, influence and intensity of chemical weathering and (iii) chemical mobility of major and trace elements during the GAP weathering.
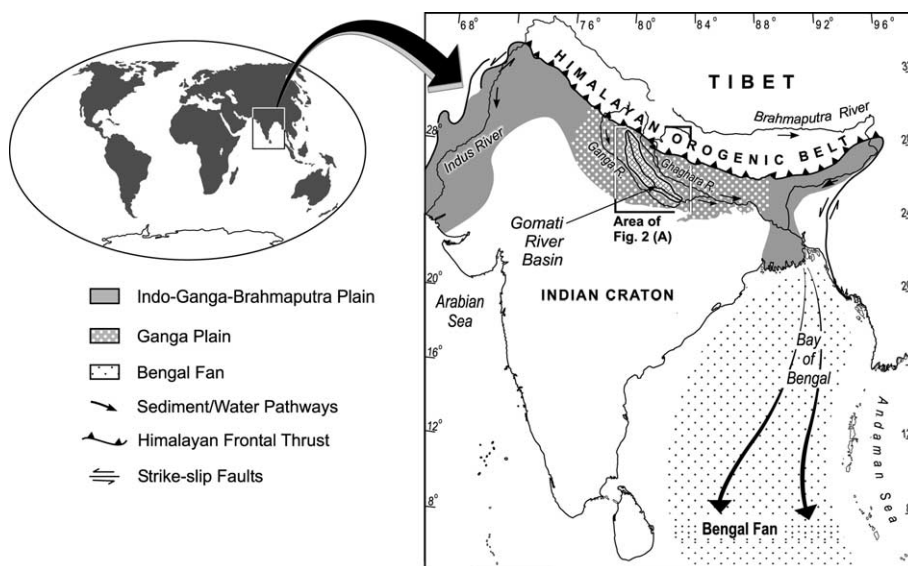

Fig. 1. Location map of study area showing the Gomati River Basin and its relation to the Ganga River system.

2. Study area

The GAP is an outstanding geographical feature on the Indian sub-continent due to its low elevation, low relief, high fertility and high population density. From North to South, Singh (1996) divided the plain into three broad distinctive units on the basis of landforms, characteristic deposits and tectonic setting: the Piedmont Zone, the Central Ganga alluvial plain and the marginal alluvial plain. The 900-km-long Gomati River originates from a swampy area in the Piedmont Zone in district Pilibhit near Puranpur, located about 50-km south of the Himalayan foothills and ultimately meets the Ganga River (Fig. 2(a)). It drains a total area of 30,437 km^2 located in an interfluve region of the Ganga and Ghaghara Rivers. It has a gently slopping elongated drainage basin trending NW–SE characterized by similar lithological and climatological conditions. The average slope of the river in its upper reaches is 55 cm/km, whereas in the lower reaches it is 11 cm/km. Maximum and minimum elevations in the basin are about 186 and 80 m above mean sea level, respectively. Thus maximum relief is approximately 25 m and is manifested by steep discontinuous exposure of the Gomati River valley margins.

Climate is an important variable that controls the geochemical environment of weathering processes and also has an overriding influence upon the characteristic weathering products (Nagell, 1962). The degree of weathering increases with mean annual temperature and precipitation. Temperature controls the rate of chemical weathering reactions and precipitation provides an aqueous medium and moisture for ion exchange for these reactions (Loughnan, 1969). The Gomati River basin experiences a humid sub-tropical climate with hot summers followed by heavy monsoon precipitation and cold winters. Annual rainfall in the region varies from 87 to 125 cm. The major part of the rainfall is concentrated in the monsoon months, July–October, with only few sporadic rains in the winter months. Variation in temperature is extreme in the summer months. Maximum temperature is 47 °C and in the winter months it is 20 °C and the minimum is about 2 °C. Fig. 2(b) shows monthly rainfall and maximum and minimum temperature at a few locations in the study area (Singh, 1988).
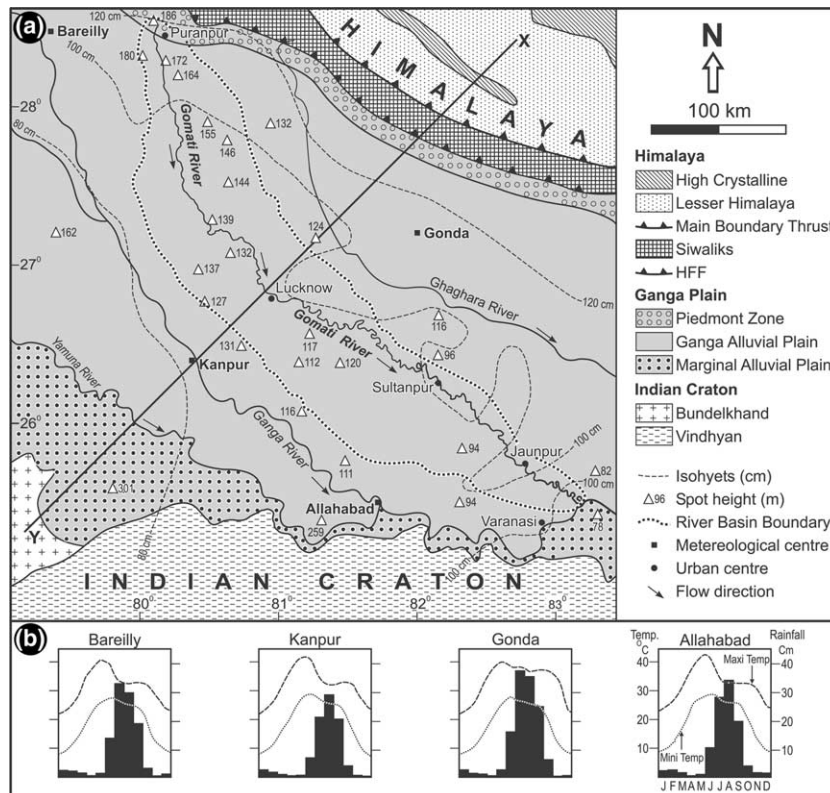

Fig. 2. (a) The Gomati River Basin: It represents the interfluve area of the Ganga and the Ghaghara Rivers in the Ganga alluvial plain and is drained by low-gradient and highly sinuous entrenched channels. Annual rainfall isolates were generalised from Singh (1988). (b) Rainfall and temperature distribution of some stations of the Ganga alluvial plain (after Singh, 1988).
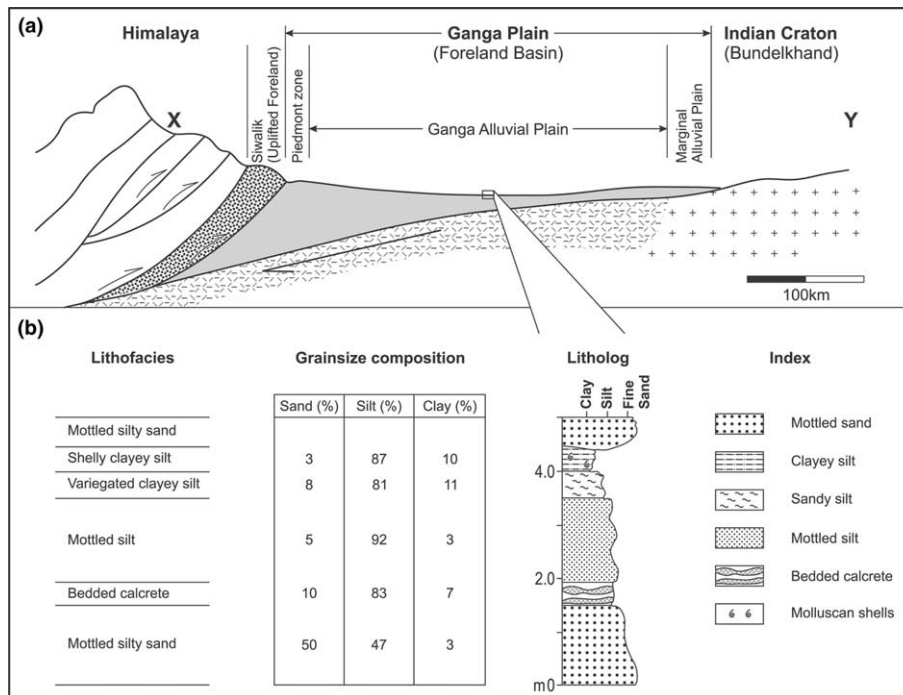
Fig. 3. (a) Schematic cross-section (along *XY* line as shown in Fig. 2(a)) showing geology and tectonic setting of the Ganga alluvial plain. (b) Schematic vertical litholog showing lithofacies and their average grainsize composition of late quaternary alluvial deposits exposed on the margin of the Gomati River valley at Lucknow (after Singh et al., 1999).

Geologically, the GAP is a foreland basin which is closely linked to the development of the Himalaya orogenic belt (Fig. 3(a)). Lithologically, the GAP is made-up of interlayered 1–2 m thick fine sand and silty mud deposits showing extensive discontinuous calcrete horizons (Singh, 1996). These sediments achieve a thickness of 500–1000 m near the foothills of the Himalaya and decrease southwards, where they may be only few tens of meters thick. Based on grainsize, contact relationships, burrowing, mottling and calcretization in the plain, Singh (1996) identified two types of lithofacies association: Muddy interfluve deposits and Sandy interfluve deposits. Sandy interfluve deposits are made up of 0.5–2.0 m thick lenticular sand bodies representing meandering river deposits and 1.0–2.0 m thick well sorted silty fine sand representing sheet flood deposits with 10–50 cm thick discontinuous horizons of calcrete. Sometimes 1.0–2.0 m thick muddy sediments representing pond-lake deposits are also present. Muddy interfluve deposits are made up of 0.2–1.0 m thick well sorted silt with extensive calcrete development; 1.0–2.0 m thick highly mottled fine sand deposits with 5–10 cm thick bedded calcrete and shell-bearing mud. An idealised vertical succession depicting these lithofacies associations along with their average grainsize characteristics near Lucknow is shown in Fig. 3(b) (Singh

et al., 1999). In the central part of the Gomati River basin, a thick section of about 8 m exposed on the Loni River near Lucknow was studied in detail for luminescence dating. This section comprises silty sediments with bands of fine sand and calcrete horizons and gave an age of 46 ± 6 ka at its base (Srivastava et al., 2003).

Hydrologically, the Gomati River is characterized by sluggish flow throughout the year, except during the rainy season when heavy monsoon rainfall causes a manifold increase in its runoff. The river has several tributaries draining through the GAP and thereby actively incorporating into its sediment load. The Sai River is the main right bank tributary which drains nearly 1/3 of the Gomati River basin. Other tributaries are the Kathna Nadi, the Sarayan Nadi, the Kalyani Nadi, the Behta Nadi, the Pili Nadi, the Loni Nadi, Kundu Nala and the Athhi Nala. The river hydrograph is highly controlled by the intensity and duration of monsoon rainfall. Annual discharge of the river is about 7390×10^6 m^3 (Rao, 1975). In the monsoon season, maximum river velocity ranges from 1.5 to 2.0 cm/s, water level increases up to 5 m and total suspended matter increases downstream from 10 to 600 mg/L. In 1871, flood records of the Gomati reported the extreme discharge of 973 m^3/s with water velocity being 1.60 m/s. During the monsoon season, weathering products from a part of the

GAP are transported by the Gomati River into the Ganga River System. Only a fraction of it gets deposited along the river as channel or over-bank/flood deposits. The annual sediment load and annual sediment erosion rate of the Gomati River basin have been reported to be 6000×10^6 kg and 225×10^3 kg/km^2, respectively (Abbas and Subramaniam, 1984).

Sedimentologically, the nature of the sediment transported by the Gomati River is very similar to those of its tributaries and is strongly controlled by the sediments available in the river basin for weathering processes. Channel sediments of the river are mineralogically identified as lithic graywacke (Kumar and Singh, 1978). Average mineral composition of the river sand includes quartz (55%), rock fragments (19%), muscovite (15%), K-feldspar (8%), biotite (2%) and plagioclase (1%). Relative abundance of clay minerals in the river sediments shows illite (61%) along with smectite (26%), kaolinite (7%) and metastable chlorite (6%) in minor amounts (Sarin et al., 1989). Mean grainsize of the bedload is very fine sand whereas the suspended load varies from coarse silt to very fine silt (Kumar and Singh, 1978; Gupta and Subramanian, 1994).

3. Sampling and analytical methods

In order to produce coherent and quantitative geochemical data, the present study depends upon the suitability, representativity and consistency of samples collected. In order to acquire geochemical variability both spatially and statistically, the sampling plan required careful consideration and was determined by the nature and availability of samples of the GAP weathering products. These weathering products are transported by the Gomati River as bedload, mixed load and suspended load and therefore, classified into three groups as channel sediments (CS), flood sediments (FS) and suspended sediments (SS). Their respective locations across the Gomati River valley are shown in Fig. 4(a). As the Gomati River hydrograph is quite peaked in the monsoon season, overall sampling duration was timed to correspond with it. Sampling was done during mid-August of 2001, representing the peak monsoon discharge of the river (Fig. 4(b)).

A set of 26 samples from the Gomati River and 2 from the Ganga River were collected at various locations as shown in Fig. 4(c). Sample locations were
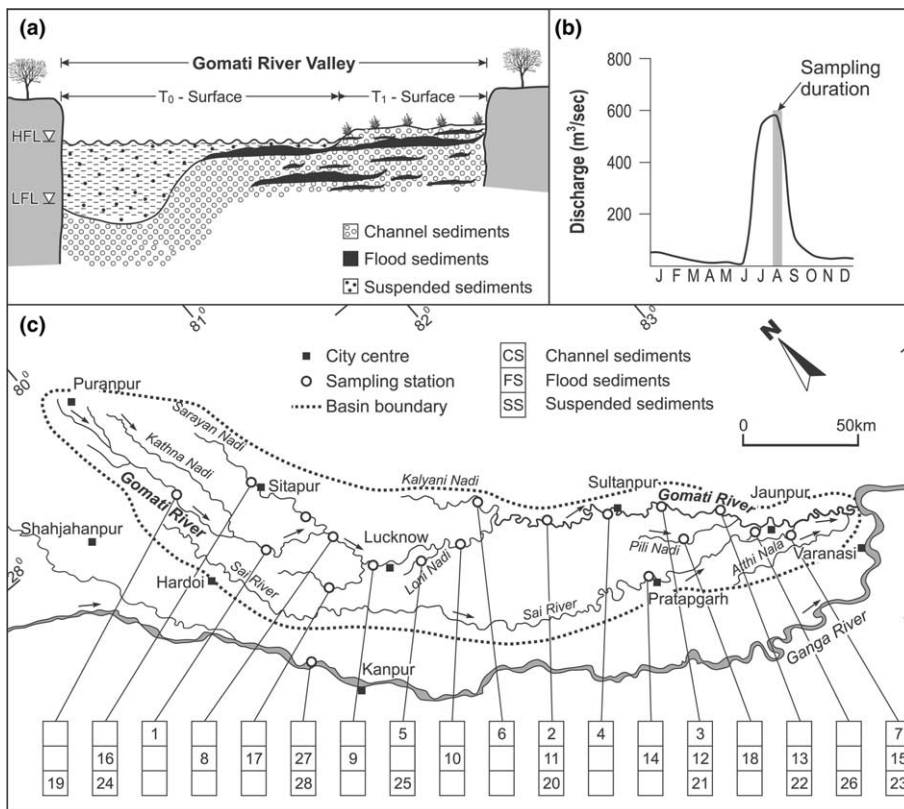

Fig. 4. (a) Schematic presentation of the Gomati River valley morphology showing-sampling plan for of the present study. (b) Schematic hydrograph of the Gomati River showing sampling duration. The river discharge is highly peaked and controlled by the monsoon. (c) Sampling sites on the Gomati River, its tributaries and the Ganga River.

carefully chosen to avoid contamination from riverbank sediments or from anthropogenic reworking activities. CS samples were taken from freshly deposited bars in the middle of the main channel or near the river margins. FS samples were collected from freshly deposited sediments of overbank deposits. SS samples were collected using a 5-L polyethylene container at a depth of 10–50 cm of active channel. All SS samples were collected from bridges near the middle of the main flowing channel. These water sample containers were kept undisturbed for a week at room temperature. SS were collected by draining away water from the containers just above level of the settled material. All sediment samples were allowed to air-dry (∼24 h) at room temperature, after which the dry sample was gently disaggregated.

The determination of major and trace element content was carried out by using a Philips PW 2400 X-ray fluorescence spectrophotometer at the laboratory of the Chair of Applied Geology at Erlangen. About 1000 g aliquots were weighed accurately and ignited in a clean ceramic crucible at 1030 °C for at least 12 h in a muffle furnace to constant weight. The samples were mixed with 1:2.5:2.5 (by weight) of spectroscopic grade Li tetraborate and Li metaborate flux, previously dried at 400 °C for 4 h. Mixing was done directly in the crucible with a small glass pestle. A few mg of I_2O_5 was added as a non-wetting agent. The mixture was then fused in Pt (95%)–Au (5%) crucibles for 10 min, the fusion being carried out with an Oxiflux® burner system. During the fusion, the crucible was regularly rotated to ensure thorough mixing of the melt while keeping an oxidising atmosphere during fusion. The molten mixture was then poured into a Pt (95%)–Au (5%) mould heated red hot with a gas burner and allowed to solidify. The mould was cooled by a stream of air thus allowing easy handling.

The 10 elements traditionally listed as oxides in the major element chemical analysis, Al, Si, Ti, Fe, Mn, Mg, Ca, Na, K and P were determined in all samples. Trace elements Ba, Ce, Cr, Cu, Ga, La, Nb, Ni, Pb, Rb, Sr, V, Y, Zn and Zr were also analysed. The precision and accuracy of the preparation and the instrumental performance of the XRF was checked using the international reference samples JSd-1, JSd-2, JLk-1, SARM-46, SARM-52, JB-2, JGb-2 and IAEA-SL-1, which are measured as 'unknowns' with samples and sample duplicates. With few exceptions, there were no discrepancies between the analytical data obtained and the consensus data in international reference samples.

4. Results

In order to gain an overall impression of major and trace element distribution in the GAP weathering products, the full array of results has been presented in Table 1. The average chemical composition of CS, FS and SS were also reported. Correlation coefficients between each pair of elements have been calculated in order to search for inter-element relationship. Data for UCC from Taylor and McLennan (1985) and World Sediments from McLennan (1995) have been discussed to facilitate the interpretation of the present geochemical study.

4.1. Major elements

Major element composition of river sediments is used to study the quantification of chemical and physical weathering, to ascertain inter-element relationships and rock classification, as well as for assessing geochemical processes operating on a river basin (Rollinson, 1993). The bulk chemistry of the Gomati River Sediments mostly consists of oxides of three elements: Al, Si and Fe. Their total composition accounts more than 90%, 80% and 75% in CS, FS and SS, respectively. The SiO_2/Al_2O_3 ratios of CS, FS and SS in the Gomati River is 9.4, 5.2 and 3.4, respectively. This strongly reflects mineral composition, in which quartz dominates in CS and clay minerals in SS. Fine-grained aluminosilicate minerals are preferentially transported as suspension load (SS) and quartz as bedload (CS). Other major elements behave like Al_2O_3. Mica, kaolinite and chlorite accounts more than 80% of clay mineral content in SS, whereas quartz accounts for more than 50% in the sand fraction of the Gomati River (Kumar and Singh, 1978; Chakrapani et al., 1995).

4.1.1. Elemental ratio

The chemical composition of weathering products of a river basin is expected to demonstrate well-established concepts on mobility of various elements during weathering processes (Berner and Berner, 1996; Stallard, 1988; Drever, 1988). The identification and evaluation of major element mobility during the GAP weathering was done with the help of elemental ratios calculated with respect to the least mobile element Al; i.e., it is believed to stay in the weathered material. The ratio of the content of element X and Al_2O_3 in the Gomati River Sediments divided by the ratio of the same element content in UCC gives the following element ratio:

$$\text{Element ratio}(X) = \frac{X/Al_2O_3 \ (\text{Gomati River Sediments})}{X/Al_2O_3 \ (\text{UCC})}.$$

This element ratio refers to the relative enrichment or depletion of the element, i.e. >1 indicates enrichment, <1 indicates depletion and = 1 indicates no change in the relative abundance of element.

Fig. 5(a) displays element ratios in CS, FS and SS of the Gomati River. As demonstrated, element ratios of FS are strongly accentuated between CS and SS due to

Table 1
Estimates of the major (in weight percent) and trace elements (in ppm) composition and loss of ignition (LOI) in channel sediments (CS), flood sediments (FS) and suspended sediments (SS) of the Gomati and Ganga Rivers

Serial number	River/ tributary	Sampling station	Sediment type	SiO$_2$	TiO$_2$	Al$_2$O$_3$	Fe$_2$O$_3$	MnO	MgO	CaO	Na$_2$O	K$_2$O	P$_2$O$_5$	LOI	SUM	Ba	Ce	Cr	Cu	Ga	La	Nb	Ni	Pb	Rb	Sr	V	Y	Zn	Zr
1.	Gomati	Nimsar	CS	82.3	0.30	8.43	1.48	0.03	0.97	0.59	1.55	2.14	0.08	1.07	98.99	321	84	38	9	10	14	8	6	25	98	86	45	21	3	236
2.	Gomati	Jagdishpur	CS	78.3	0.38	9.45	2.46	0.04	1.07	1.00	1.50	2.48	0.10	2.17	98.98	369	80	46	17	13	20	9	15	24	130	86	61	23	24	210
3.	Gomati	Chanda	CS	81.2	0.26	7.95	1.71	0.05	1.56	0.67	1.45	2.00	0.09	1.65	98.62	299	81	43	14	10	15	7	7	21	88	81	60	23	1	129
4.	Gomati	Sultanpur	CS	80.9	0.53	8.46	2.00	0.04	1.36	0.79	1.51	2.07	0.14	1.44	99.22	314	232	47	14	11	39	12	9	23	100	90	53	46	16	567
5.	Loni	Gangaganj	CS	73.1	0.45	8.86	2.69	0.04	3.52	2.10	1.29	2.18	0.09	4.77	99.14	353	81	52	12	13	18	9	13	18	109	94	61	25	24	245
6.	Kalyani	Masauli	CS	80.4	0.37	8.32	1.91	0.03	1.14	0.80	1.40	2.11	0.08	1.99	98.58	357	104	44	17	11	25	9	11	22	96	88	49	25	10	275
7.	Sai	Jaunpur	CS	83.0	0.32	7.75	1.63	0.03	0.97	0.66	1.35	2.01	0.07	1.66	99.46	309	98	36	2	10	12	7	7	22	92	76	44	21	14	235
	GRB	Average	CS	79.9	0.37	8.46	1.98	0.04	0.94	1.51	1.44	2.14	0.09	2.11	99.00	332	109	44	12	11	20	9	10	22	102	86	53	26	13	271
8.	Gomati	Itonja	FS	74.4	0.53	11.45	3.38	0.07	1.15	1.32	1.44	2.81	0.10	3.32	99.97	460	91	46	14	14	41	14	21	29	157	90	44	38	52	300
9.	Gomati	Lucknow	FS	68.4	0.66	12.97	4.37	0.07	1.31	1.94	1.31	3.15	0.09	4.59	98.86	516	97	68	22	18	33	16	35	25	176	93	60	35	67	259
10.	Gomati	Nepuraghat	FS	70.0	0.57	11.89	3.92	0.06	2.00	2.01	1.30	2.92	0.13	5.00	99.80	470	80	59	13	16	30	14	23	21	157	92	47	32	65	269
11.	Gomati	Jagdishpur	FS	71.3	0.62	11.95	3.93	0.06	1.85	1.89	1.52	2.89	0.13	4.55	100.69	482	102	64	20	16	44	15	27	26	156	96	49	36	64	338
12.	Gomati	Chanda	FS	69.0	0.57	10.92	3.71	0.06	3.11	2.43	1.26	2.66	0.14	5.85	99.71	427	86	55	20	16	35	14	24	25	139	95	47	31	63	326
13.	Gomati	Budalpur	FS	67.0	0.69	13.48	4.80	0.08	1.58	2.15	1.18	3.20	0.12	5.39	99.67	509	97	81	19	18	32	16	34	34	171	95	61	38	77	280
14.	Sai	Pratapgarh	FS	63.6	0.71	14.00	5.14	0.08	1.95	2.44	1.17	3.22	0.10	6.88	99.29	517	89	84	21	18	30	15	38	26	176	107	63	35	83	231
15.	Sai	Jaunpur	FS	65.8	0.64	12.70	4.56	0.07	2.57	2.42	1.18	3.00	0.11	6.44	99.49	476	58	73	20	17	30	14	32	26	161	101	55	36	69	275
16.	Sarayan	Konighat	FS	60.6	0.68	14.18	5.43	0.08	2.57	2.81	1.11	3.37	0.15	8.44	99.42	521	88	82	28	19	29	15	41	33	188	104	62	34	92	201
17.	Sai	Malihabad	FS	58.2	0.71	15.23	5.97	0.10	2.33	3.02	0.93	3.74	0.13	8.26	98.62	595	68	87	28	20	27	15	43	35	207	87	68	36	96	199
18.	Pili	Badalpur	FS	67.3	0.59	12.51	4.36	0.07	2.37	2.38	1.14	3.03	0.10	5.96	99.81	501	73	62	16	16	32	14	28	29	162	91	48	35	67	235
	GRB	Average	FS	66.9	0.63	12.84	4.51	0.07	2.26	2.07	1.23	3.09	0.12	5.88	99.58	498	84	69	20	17	33	15	31	29	168	96	55	35	72	265
19.	Gomati	Nepuraghat	SS	53.6	0.64	14.99	5.87	0.09	4.96	4.44	1.27	3.69	0.15	10.61	100.31	540	62	84	28	22	21	14	43	27	193	101	65	36	99	162
20.	Gomati	Jagdishpur	SS	52.7	0.66	15.80	6.24	0.10	4.12	4.14	1.37	3.89	0.15	9.47	98.64	572	81	98	36	23	26	14	148	36	207	95	76	35	106	151
21.	Gomati	Chanda	SS	53.6	0.71	16.51	6.6	0.11	3.21	3.8	1.03	3.93	0.16	10.41	100.07	578	57	94	40	20	25	17	48	35	210	99	73	37	110	154
22.	Gomati	Budalpur	SS	54.4	0.68	15.45	6.16	0.10	3.79	3.86	1.43	3.77	0.15	10.29	100.08	568	75	90	58	20	19	15	49	36	202	121	73	36	101	160
23.	Sai	Jaunpur	SS	53.5	0.71	14.99	6.00	0.10	3.56	3.48	2.63	3.52	0.13	11.60	100.22	558	74	97	56	20	22	15	56	30	193	145	76	37	101	181
24.	Sarayan	Konighat	SS	54.3	0.72	16.21	6.59	0.11	3.06	3.77	1.29	3.90	0.14	10.11	100.20	588	77	96	40	21	21	16	63	40	207	100	78	34	109	152
25.	Loni	Gangaganj	SS	54.0	0.62	14.87	5.61	0.08	5.17	4.45	0.98	3.72	0.13	10.25	99.88	552	71	78	26	20	20	16	34	28	185	90	60	34	84	160
26.	Kandu	Jaunpur	SS	51.8	0.70	15.42	6.23	0.09	3.27	3.84	2.59	3.66	0.12	13.24	100.96	558	81	105	65	20	21	15	55	31	205	153	84	32	129	148
	GRB	Average	SS	53.5	0.68	15.53	6.16	0.10	3.97	3.89	1.57	3.76	0.14	10.75	100.05	564	72	93	44	21	22	15	62	33	200	113	73	35	105	159
27.	Ganga	Bilhaur	FS	63.9	0.69	13.76	5.12	0.08	2.41	2.86	1.29	3.18	0.12	5.94	99.35	514	76	70	25	20	34	16	32	27	164	83	62	40	78	227
28.	Ganga	Bilhaur	SS	59.2	0.69	15.76	5.99	0.10	2.59	3.16	1.27	3.73	0.14	7.20	99.83	580	85	82	48	23	28	16	43	40	198	92	75	40	103	176
	World Sediment*			64.2	0.75	13.42	5.72	0.09	3.07	8.95	1.68	2.83	0.15	–	100.8	480	59	74	40	16	28	17	40	17	110	385	110	21	65	210
	Upper continental crust**			65.9	0.50	15.19	5.00	0.08	2.21	4.2	3.90	3.37	0.16	–	100.5	550	64	35	25	17	30	25	20	20	112	350	60	22	71	190

S. No. refers to sample locations on Fig. 4. GRB refers the Gomati River Basin.
* Data from McLennan (1995).
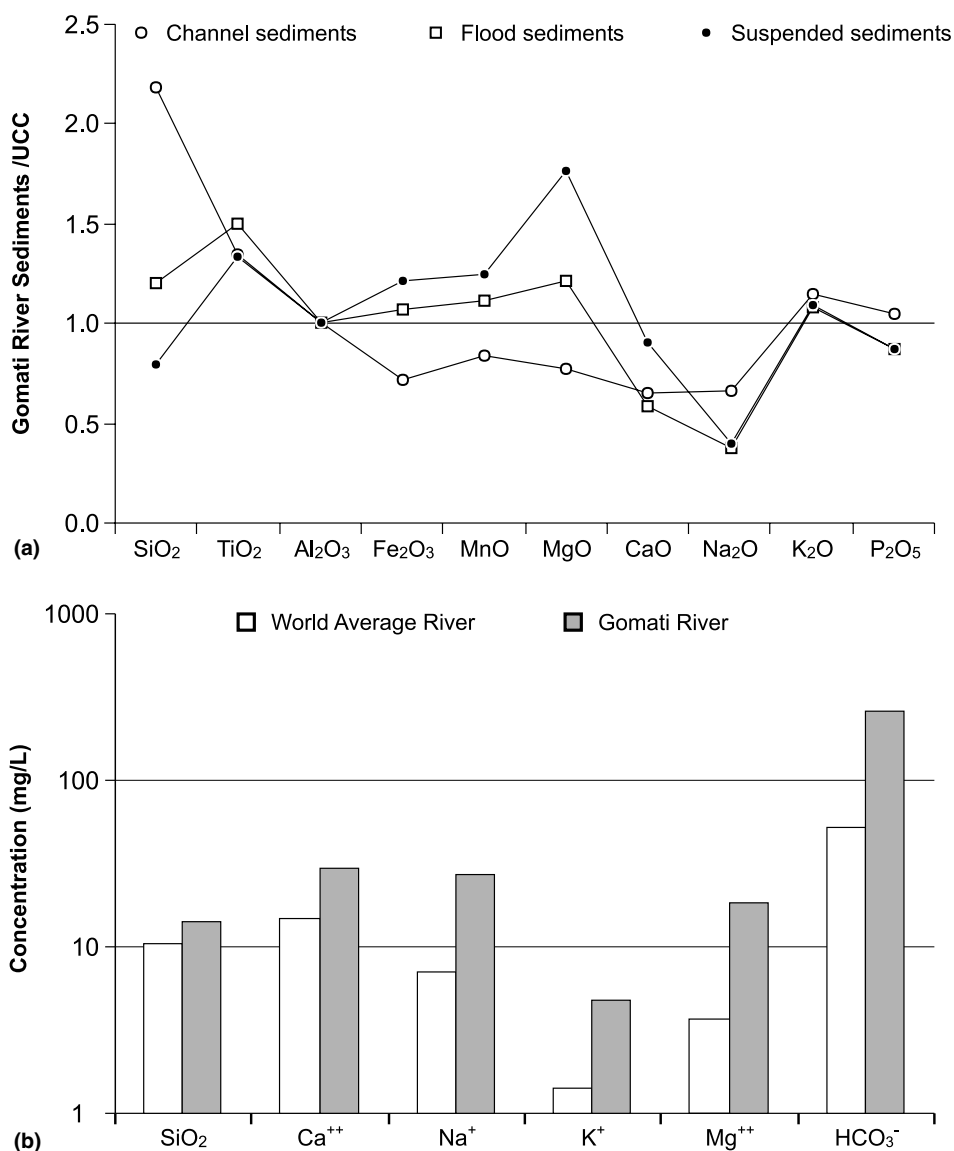** Data from Taylor and McLennan (1985).

Fig. 5. (a) Element ratio of channel, flood and suspended sediments of the Gomati River, calculated from average major element concentrations normalised to UCC (Taylor and McLennan, 1985) with respect to Al_2O_3. This graph clearly shows the enrichment of SiO_2 in channel sediments, MgO in suspended sediments and TiO_2 in all sediment types. (b) Bar diagram displays increased elemental composition of the Gomati River water with respect to average World River Water (Berner and Berner, 1987).

their granulometric nature. The mobility of SiO_2 is critical for an understanding of chemical weathering, soil formation and distribution of elements in natural waters. The SiO_2 content is markedly enriched in CS and depleted in SS. Titanium is considered as relatively immobile and is markedly enriched in all domains of the Gomati River Sediments. Whereas the highly mobile elements Ca and Na show relative depletion. Potassium is considered separately as less mobile than the mobile elements and remains slightly enriched. In contrast to Na,

K is preferentially adsorbed by clay minerals in the sediments. Silicate minerals formed during weathering or alteration of pre-existing clays (montmorillonite to mixed layers) incorporate K in preference to Na despite the greater abundance of Na in the Gomati River water. Magnesium and K become tightly incorporated in the clay minerals instead of Na and therefore, show pronounced enrichment in SS and FS. Depletion of Na and Ca may have been caused due to their highly mobile nature during chemical weathering as a result of which

they have become enriched in the dissolved load of the Gomati River water. Magnesium readily dissolves in weathering solutions, enters into the aqueous phase and becomes concentrated into SS. Its depletion in CS indicates its mobility into SS and FS. Sarin et al. (1989) shows that the water chemistry of Himalayan rivers is dominated by carbonate weathering, in which Ca + Mg account for 80% of the cations. SS and FS, therefore, show prominent Mg enrichment compared to other major elements.

Monsoon-derived rainwater reacts with the GAP forming minerals and calcrete carbonates. During mineral weathering, SiO_2, Na and K ions originate by incongruent dissolution of feldspars. Magnesium and K are released by weathering of biotite and ferromagnesium minerals. Calcium may also be derived from dissolution of calcrete bands. Silica enters into the river water during weathering of silicate minerals except quartz. These SiO_2, Ca, Mg, Ca, K and Na ions are preferentially removed by solution (Nesbitt et al., 1980) and, therefore, show a distinct enrichment in the Gomati River water compared to the world average river water. Fig. 5(b) displays a bar diagram of river water composition of the Gomati along with world average values (Berner and Berner, 1987).

Major elements ratios of Al_2O_3/SiO_2 and Fe_2O_3/SiO_2 of the Gomati River Sediments were plotted with respect to the Himalaya and the Siwalik. Mean chemical composition of the Himalaya is relatively similar to that of average UCC (Galy and France-Lanord, 2001). The linear trend of CS and SS indicate the enrichment of quartz content in CS and of phyllosilicates in SS by mineral sorting response during fluvial transportation and deposition (Fig. 6). It is interesting to note that the elemental ratios of river sediments collected from delta region of the Ganga and the Brahmaputra Rivers is quite similar to that of the present study (Galy and France-Lanord, 2001). The lower ratios of CS in the Gomati River with respect to the Siwalik and the Himalaya indicate the increase of compositional maturity of the river sediments in the GAP weathering.

4.1.2. Inter-element relationship

Fig. 7 displays inter-element relationships plotted on variation diagrams using Al_2O_3, SiO_2 and TiO_2 along the *x*-axis. The linear trends from CS, FS and SS were observed with strong positive or negative correlations. Strong negative correlation of SiO_2 with all other major elements indicates grainsize control on the geochemistry of the GAP weathering products. The increasing trend of TiO_2 with Fe_2O_3 is attributed to the enrichment of heavy minerals in SS. However, MgO and K_2O have different patterns with Al_2O_3 and TiO_2, respectively. The correlations of CaO with others are highly variable due to dissolution of calcrete layers present within the alluvial sequence of the GAP.
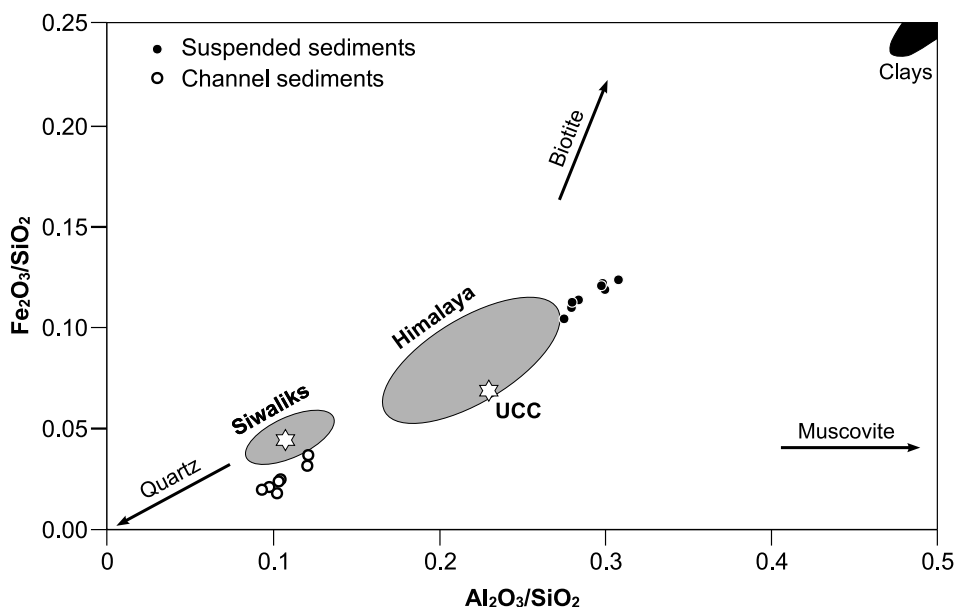

Fig. 6. Al_2O_3 /SiO_2 versus Fe_2O_3/SiO_2 for river sediments of the Ganga alluvial plain along with the Siwaliks and the Himalayan sources. Lower ratios for CS and higher ratios for SS indicate increase of the quartz proportion and enrichment of phyllosilicates, respectively. Linear trend corresponds to mineralogical sorting of these sediments during fluvial transportation. Gray ellipses indicate composition of source area: the Himalaya and the Siwaliks (Galy and France-Lanord, 2001). Star corresponds to average UCC (Taylor and McLennan, 1985).
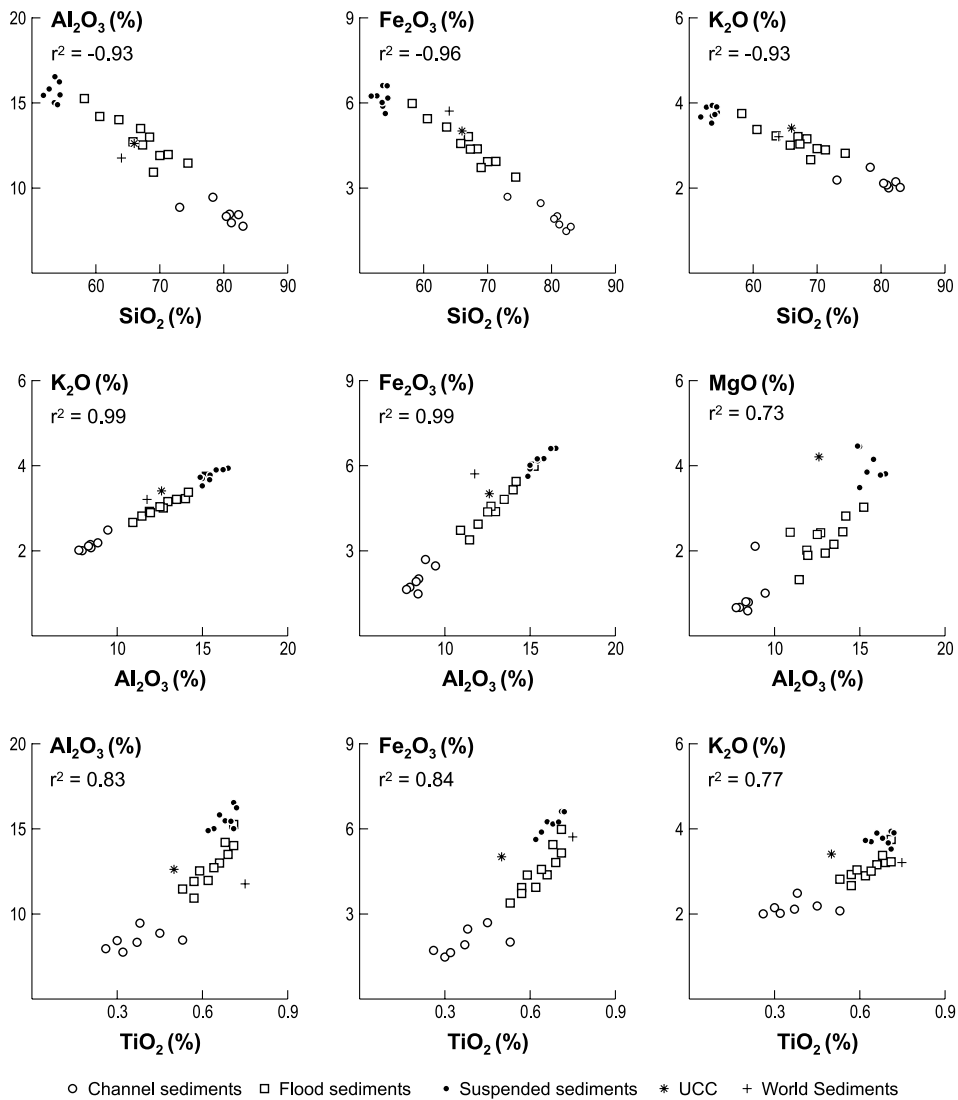
Fig. 7. Selected variation diagrams of major elements in channel, flood and suspended sediments of the Gomati River are plotted against Al_2O_3, SiO_2 and TiO_2. Note that mineral sorting in fluvial transportation and deposition is the single important factor that strongly influences distribution of major elements in these sediments. For reference, UCC and World Sediments were also plotted as star and cross, respectively (Number of samples = 26).

Plotting the chemically immobile TiO_2 against SiO_2 provides further insight into chemical and hydrodynamic behaviour of the major mineral phases and indicates that they were concentrated into the fine-grained sediment fraction (SS). High concentrations of TiO_2 in SS and a strong correlation with Al_2O_3 and K_2O indicate that Ti was derived from mica in the Gomati River Sediments. Titanium oxide vs. Fe_2O_3 displays a good correlation ($r^2 = 0.84$) indicating their common sources from ferromagnesium minerals such as biotite, amphibole, pyroxene, etc. A good correlation of K_2O with MgO and Al_2O_3 indicates a common source from illite, the dominant clay mineral present in SS. A good corre-

lation of Fe_2O_3 with Al_2O_3 may be associated with alteration of biotite into aluminosilicates and Fe(III) oxides. All these relationships suggest that the distribution of major elements in the GAP weathering products have strong inter-elemental linkage.

4.1.3. A–CN–K diagram and chemical index of alteration

Nesbitt and Young (1982) proposed the quantification of chemical weathering intensity expressed as a "chemical index of alteration" (CIA) where:

$$CIA = [Al_2O_3/(Al_2O_3 + CaO^* + Na_2O + K_2O)] * 100.$$

Using molecular proportions and with CaO* representing CaO in silicates only (Nesbitt and Young, 1989; Nesbitt et al., 1996). A CIA value of 100 indicates intense chemical weathering along with complete removal of all the alkali and alkaline earth elements, whereas CIA values of 45–55 indicate virtually no weathering. Average UCC and unaltered granite rocks have a CIA value of about 47 and 50, respectively. It is necessary to make a correction to the measured CaO content for the presence of Ca in carbonates and phosphates. This is normally accomplished by calculating corrections from measured CO_2 and P_2O_5 contents. Where such data are not available, approximate corrections can be made by assuming reasonable Ca/Na ratios in silicate material. In this study, the CaO content was corrected for phos-

phate using available P_2O_5. If the remaining number of moles is less than that of Na_2O, this CaO value was adopted. If the number of moles is greater than Na_2O, CaO* was assumed to be equivalent to Na_2O. Since Ca is typically lost more rapidly than Na during weathering, it will give minimum (by up to about 3 units) CIA values. Discrepancies are likely to be greatest for intermediate CIA values (60–80 units).

Data are plotted on ternary A–CN–K diagram along with the location of important rock-forming minerals, UCC (Taylor and McLennan, 1985) and natural waters. Plots of CS, FS and SS tend towards the Al_2O_3 apex, showing a marked loss in Na and Ca during weathering compared to the UCC. As seen in Fig. 8(a), plots of the Gomati River Sediments display a trend of weathering
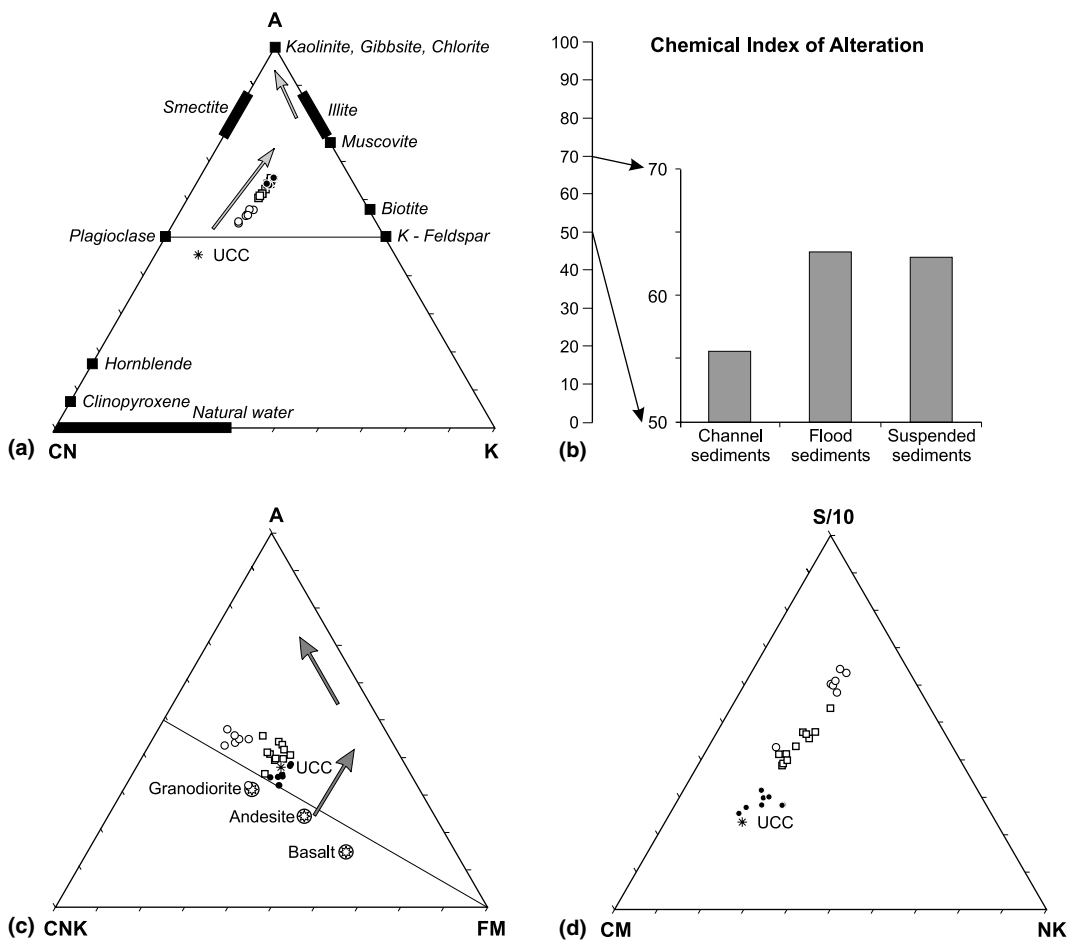
Fig. 8. (a) A–CN–K ternary diagram of molecular proportions showing sediment suites from the Gomati River. A = Al_2O_3; C = CaO; N = Na_2O and K = K_2O. Also plotted is the UCC (Taylor and McLennan, 1985) as well as idealised mineral compositions. Arrow indicates predicted weathering trends exhibited by the Ganga alluvial plain, which had experienced incipient to moderate chemical weathering. (b) Bar diagram indicates average Chemical Index of Alteration values of the Gomati River Sediments. (c) A–CNK–FM and (d) S/10–CM–NK ternary diagrams showing sediment suites from the Gomati River. A = Al_2O_3; C = CaO; N = Na_2O; K = K_2O; F = Total Fe; M = MgO; S = SiO_2. Note that Fe-oxyhydroxides and biotite have been enriched in suspended sediments and sorting concentrates quartz in channel sediments. Symbols as used in Fig. 7.

direction parallel to the A–CN line. As chemical weathering progresses, clay minerals are produced at the expense of feldspars and other minerals, and bulk composition of sediments evolve up the A–CN–K diagram along the predicted weathering trend. SS plots, highest on the diagram, reflect the predominance of clay minerals. Sodium and Ca are released first during feldspar weathering as they are less stable, but are not retained by the clay minerals of the SS and FS, and get lost to weathering solutions. Potassium released by feldspar weathering is mostly retained by the clay minerals in FS and SS. Retention of K and loss of Ca and Na during the increasing degree of chemical weathering leads to a rise in K_2O content and gives a trend parallel to the A–CN line. This might be the reason why the Gomati River Sediments collected from the different hydrological regimes show an A–CN parallel-weathering trend. Plots of very fine-grained CS are close to the feldspar line due to the effect of hydrodynamic sorting of clay minerals preferentially differentiated in FS and SS. SS plot along the upper regions of the predicted weathering trend. Two plots of SS show values close to CS. This may have been caused due to movement of the CS in suspension during high flows in monsoon discharge of the river. It also illustrates the effect of mineral and sediment sorting on major element composition of the sediments.

CIA values of CS, FS and SS of the Gomati River range between 53 and 58, 59 and 68 and 55 and 68, respectively. The Average CIA of SS and FS are higher compared to CS of the Gomati River (Fig. 8(b)). This depends on the availability and nature of the GAP weathering products for fluvial transport during the monsoon. Therefore, sediments of the Gomati River depict incipient to moderate chemical alteration intensity in the GAP weathering under a humid sub-tropical climate.

4.1.4. A–CNK–FM and S/10–CM–NK Diagrams

The weathering trend of the GAP was also observed on A–CNK–FM and S/10–CM–NK triangular plots (Nesbitt and Young, 1989). In the A–CNK–FM diagram (Fig. 8(c)), the shift of SS with high values towards the FM apex suggests the influence of secondary sedimentary processes concentrating heavy minerals in the sediments. Plots of CS were closer to feldspar composition than other sediments. During weathering, fine-grained material such as Fe-oxyhydroxides and biotite probably have been winnowed and enriched in SS. In the S/10–CM–NK diagram (Fig. 8(d)) SS plot towards the CM apex and CS towards the S/10 apex, reflecting an increase and decrease of quartz in CS and in SS, respectively. Plots were characteristically parallel to the S/10–CM line, indicating the control of Na and K mobility in these sediments during weathering. These plots also give information about the modification of

sediment composition of the GAP in a moderate chemical weathering environment under a humid sub-tropical climate towards clay minerals.

4.1.5. Rock classification

Identification of mature and immature sediments can easily be done on the basis of chemical classification of sedimentary rocks. For example, the Na_2O/K_2O ratio represents an index of chemical maturity (Pettijohn et al., 1972). In the same way, other chemical parameters are also used for characterization of sediments and sedimentary rocks. The SiO_2/Al_2O_3 ratio, the most commonly used parameter, reflects an abundance of quartz and feldspar along with clay minerals (Potter, 1978). The Fe_2O_3/Al_2O_3 ratio is successfully used as a measure of mineral stability as well as in the classification of arkose (Herron, 1988). These parameters were applied to the CS, FS and SS of the Gomati River and were plotted for different areas using the scheme from Pettijohn in Fig. 9(a) and Herron in Fig. 9(b). Both Pettijohn and Herron diagrams distinguish clastic weathering products of the GAP as arkose to litharenite and are effective in distinguishing CS, FS and SS. Kumar and Singh (1978) also reported a high percentage of feldspar and rock fragments in the CS of the Gomati River.

4.2. Trace elements

Trace elements in sediments of a river basin results from the competing influences of provenance, weathering, diagenesis, sediment sorting and the aqueous geochemistry of the individual elements. (Rollinson, 1993). Zirconium is one of the most useful elements for provenance characterisation as it is least soluble, relatively immobile and transported as a terrigenous component. In the Gomati River Sediments, high concentrations of trace elements in SS with regard to their solubilities were observed. The absolute and relative abundance of these elements in SS may be controlled by the hydrochemical characteristics (pH 7.5–8.6) along with the important role of colloids and adsorption processes on clay minerals, Al hydroxides etc of the Gomati River. These high concentrations in SS (clay-rich sediments) support the importance of geochemical investigations of the fine-grained lithologies of sedimentary sequences.

4.2.1. Elemental ratios

In the above river sediment analysis, the effect of physical sorting of sediments is still predominant on trace element concentrations. The Gomati River Sediments were normalised with respect to UCC and displayed in a multi-element diagram for elemental enrichment or depletion (Fig. 10). Differences between CS and SS are strongly accentuated with regard to FS in elements such as Cr, Ni, Cu, Zn, Ga, Rb, Ba and La. Chromium, Y, Pb, Ga, Rb and La are enriched in
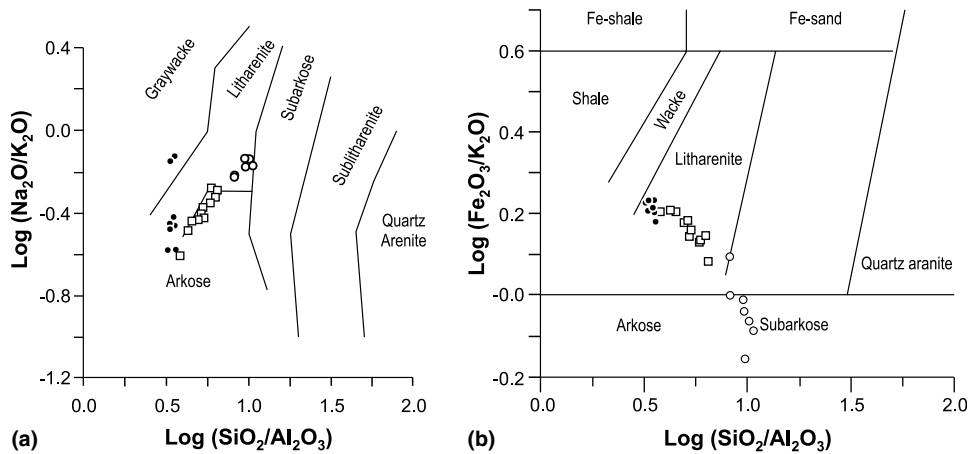
Fig. 9. Geochemical classification diagrams of the Gomati River Sediments from (a) Pettijohn et al. (1972) and (b) Herron (1988). Symbols as used in Fig. 7.
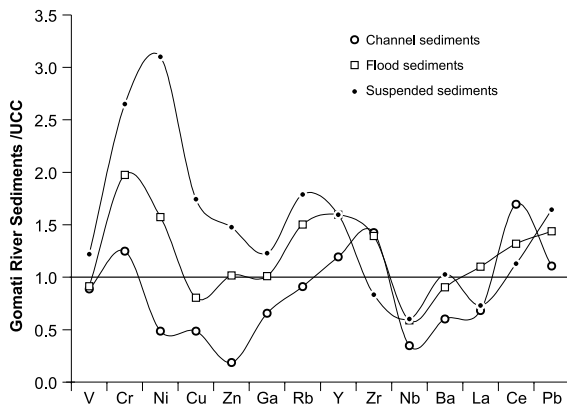

Fig. 10. Line diagram showing average trace element concentrations of the Gomati River Sediments normalised to UCC (Taylor and McLennan, 1985). Elements are plotted from left to right in order of increasing atomic number. Note the enrichment of Zr and Ce in channel sediments of the Gomati River. (Number of samples = 26).

CS and depleted in FS or SS of the Gomati River. Sediment sorting results in the enrichment of heavy minerals (zircon, monazite, magnetite, etc.) in coarse sediment fractions. Thus, the GAP weathering process tends to strongly enrich CS in such minerals and is, therefore, responsible for enrichment of Cr, Y, Zr and Ce in CS. Lead shows enrichment in all sediment fractions and may be affected by anthropogenic activities in the GAP.

4.2.2. Inter-element relationship

The minor element pairs, such as Ba–Co, Ba–Cr, Ba–Ga, Ba–Rb, Ba–V, Co–Cr, Co–Ga, Co–Rb, Co–V, Co–Zn, Cr–Ga, Cr–Rb, Cr–V, Cr–Zn, Ga–Rb, Ga–V, Ga–Zn, Rb–V and V–Zn, show very strong correlation coefficients ($r^2 > 0.90$) indicating their common sources

in the Gomati River Sediments. Fig. 11 displays some of these inter-relationships plotted on variation diagrams to facilitate the interpretation of physical sorting of sediments and its relation to trace element concentrations. Linear trends from CS and FS to SS were observed, verifying the strong influence of grainsize and mineralogy on their concentrations. For example, Zr does not show notable correlation with other trace elements except a strong positive correlation with Th indicating their common source from the heavy mineral zircon present in the sediments.

4.3. Major and trace elements

4.3.1. Extended diagrams

World Sediment normalised patterns for CS, FS and SS of the Gomati River are presented in Fig. 12(a). SS show enrichment in CaO, K_2O, Cr. Ni, Zn, Rb Y and Ce; and depletion in MgO, V, Sr and Zr. Except for Si and Zr, most other elements are considerably depleted in CS. The enrichment of Pb in all sediment domains may be due to anthropogenic activities in the GAP. The use of clastic sediment compositions in determining World Sediment composition can only give satisfactory results when various sediment types and fractions are considered in their correct relative proportions. Fig. 12(b) shows average major and trace element concentrations in SS normalised to average CS of the Gomati River and SS of the Ganga River. This diagram shows the enrichment of Fe, Ca, Mg, Ni, Cu and Zn in SS with respect to CS. The Ganga River normalised pattern is nearly flat, showing enrichment with Mg, Ca and Ni.

4.3.2. Inter-element relationship

The trace elements Ba, Co, Cr, Cu, Ga, Rb, V and Zn display moderate to strong negative correlations with
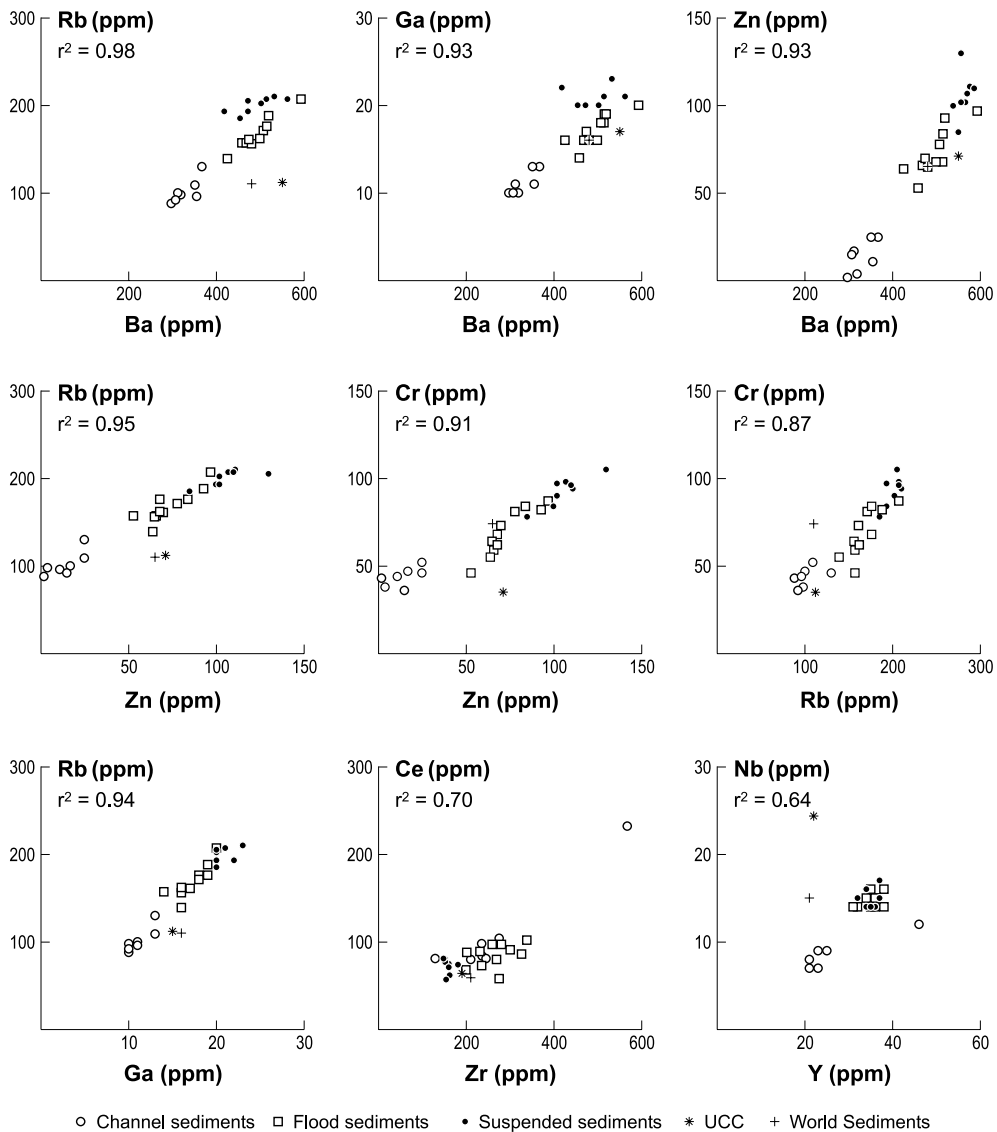
Fig. 11. Selected variation diagrams of trace elements in the Gomati River Sediments, showing role of sediment sorting in the linear clustering of plots. Note that the suspended sediments show higher trace element concentrations than in channel and flood sediments. For reference, UCC and World Sediments were also plotted as star and plus, respectively. (Number of samples = 26).

SiO_2 and positive correlations with Al_2O_3. A series of plots for some of these relations is displayed in Fig. 13. They all show linear relationships with major elements indicating that trace elements are more enriched in fine silt and clay-sized fractions than sand-fractions of the sediments. It indicates that the abundance of trace elements is controlled by the same processes that control major element distributions in the Gomati River sediments. This is in an agreement with the control by the quartz content in CS and clay minerals in FS and SS.

A good correlation of Zn with major elements (Al_2O_3, Fe_2O_3, MgO and K_2O) indicates its common source in the smectite member *sauconite*, which is characterized by the presence of Al, Mg, Fe and Zn in the lattice (Deer et al., 1966). Nickel is often co-precipitated with Fe and Mn oxides, and Zn and Ni, are both highly enriched in the SS as shown in Fig. 12(b) and shows good correlation with Fe and Mg oxides. They are also markedly depleted in CS and FS. Reaction with aqueous carbonates allows Zn and Ni to remain in solution and hence be rapidly removed by fluvial transportation during the GAP weathering. Zinc is an essential trace element for growth, development and reproduction in all-living
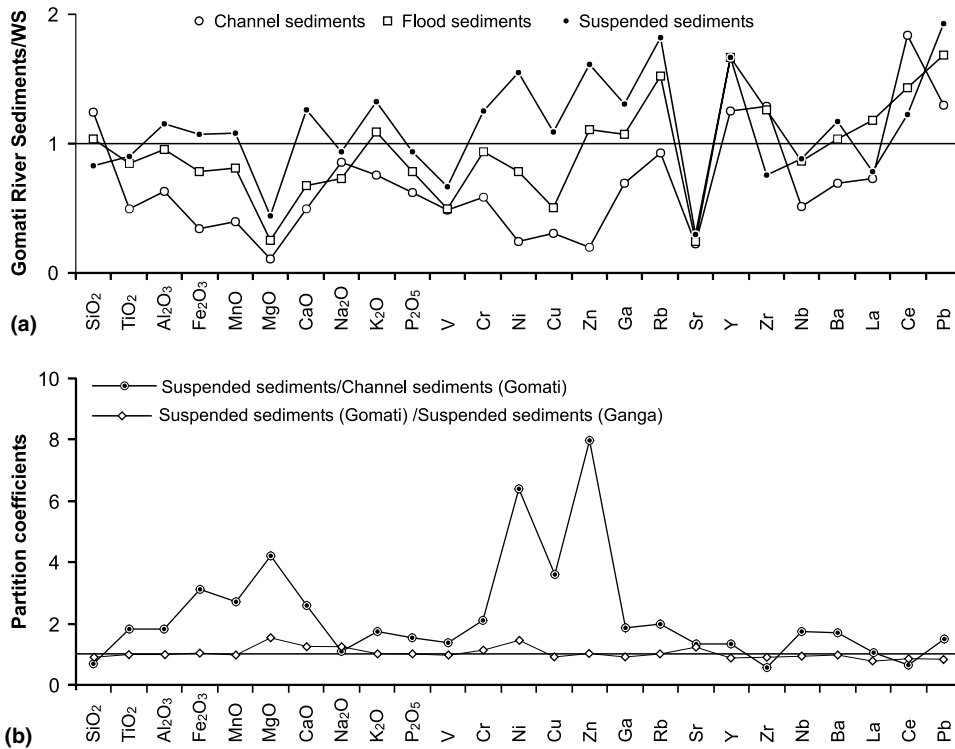
Fig. 12. (a) World Sediments normalised extended patterns of channel, flood and suspended sediments of the Gomati River. (b) Average major and trace element concentrations of suspended sediments of the Gomati River were normalised to channel sediments of the Gomati River and suspended sediments of the Ganga River. This diagram points out strong enrichment of Ni, Cu and Zn in suspended sediments of the Gomati River.

systems of the biosphere and may support the bio-productivity of the GAP.

4.3.3. Chemical mobility

Weathering is primarily a function of the mobilisation, fractionation and redistribution of major and trace elements. It is affected by various processes such as dissolution of primary minerals, formation of secondary minerals, redox processes, transportation of material, co-precipitation and ion exchange on various minerals (Chesworth et al., 1981; Nesbitt et al., 1980; Fritz and Mohr, 1984). Titanium is relatively immobile during weathering (Nesbitt, 1979) and consequently is chosen for calculation of chemical mobility of major and trace elements. It was evaluated in terms of percentage increase and decrease of element X and was calculated as follows:

$$\text{Percentage change} = \{(X/TiO_2)_{sample}/(X/TiO_2)_{UCC} - 1\}.$$

The percentage change of elements relative to TiO_2 was plotted against the CIA. These diagrams provide a basis for assessing increase or decrease in chemical mobility during progressive chemical weathering of the GAP. Sil-

icon, Na and K show a decreasing trend of chemical mobility (Fig. 14(a), (g) and (h)). Sodium decreases more rapidly than K, basically indicating greater alteration of plagioclase as compared to K-feldspar. The significant increasing trends of Fe and Mg reflect instability of biotite and muscovite as the bulk of these elements are located in these minerals which alter rapidly during the GAP weathering (Fig. 14(c) and (e)). The chemical mobility of Rb is closely linked with K, but its decrease is less than K (Fig. 14(s) and (h)). K-feldspar is known to contain more Rb than biotite and also weathers less readily than biotite. Rubidium, therefore, is expected to be less depleted than K. Barium is concentrated in K-feldspar and its chemical mobility is most similar to that of K (Fig. 14(j)).

In Fig. 14(w), Zn shows a distinct increasing trend of chemical mobility. Most of the Zn is present in biotite that rapidly alters during the GAP weathering. The enrichment of Zn is due to its incorporation or adsorption on authigenic clay minerals. The enrichment of Zn in SS of the Gomati River Sediments is most striking. Maximum concentration of Zn is found to be as high as 100 ppm. The enrichment of these elements with respect to TiO_2 may not be caused by an accumulation
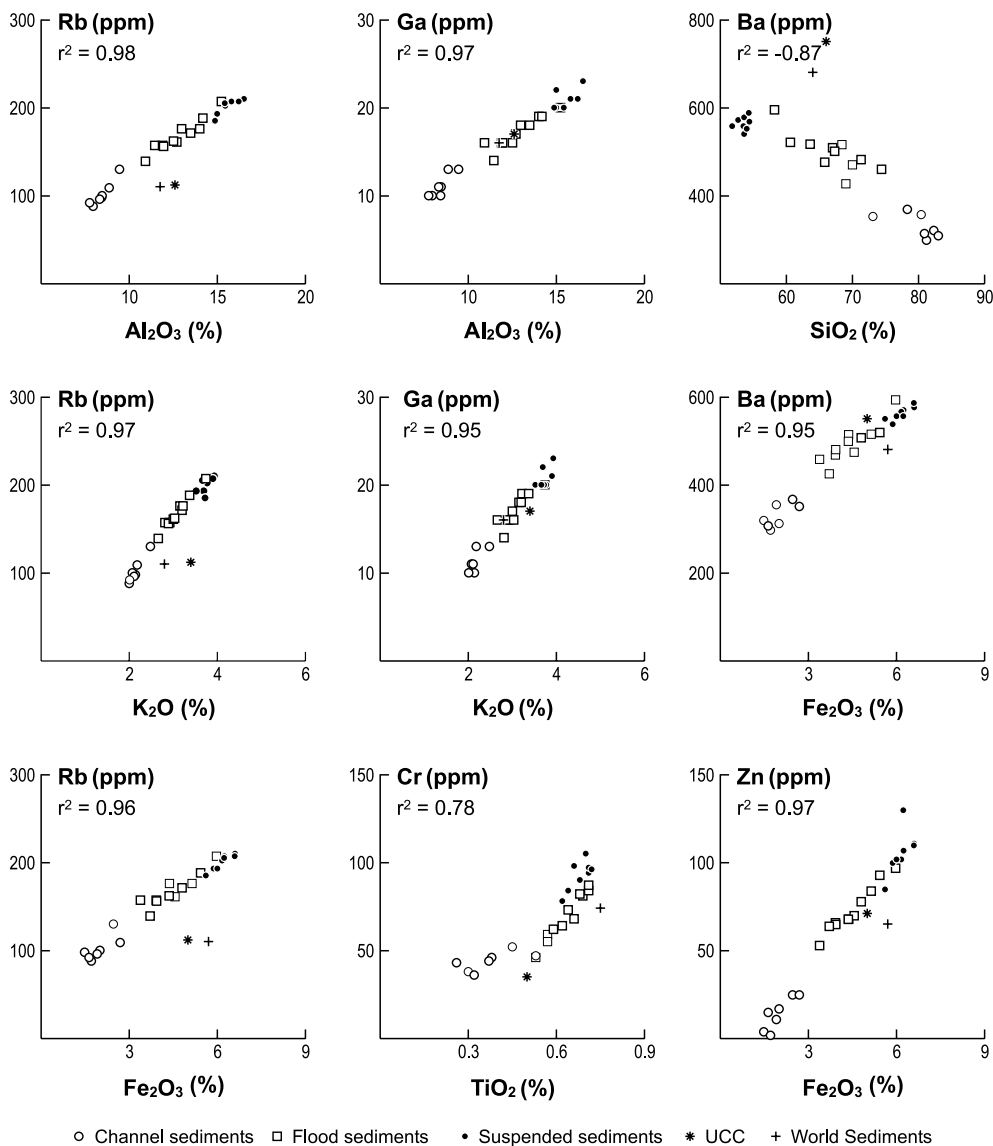
Fig. 13. Selected variation diagrams of major-trace elements in the Gomati River Sediments. For reference, UCC and World Sediments were also plotted as star and plus, respectively. (Number of samples = 26).

of resistant minerals, but results from sorption and co-precipitation processes (Middelburg et al., 1988). Zirconium, commonly assumed to be immobile, shows a decreasing trend of chemical mobility during the GAP weathering (Fig. 14(x)).

5. Weathering dynamics

Physical and chemical weathering processes both work together in normal circumstances and are determined by many factors such as lithology, topography, climate, tectonics, vegetation and biological activity (Ollier, 1984). In the GAP, these weathering processes are largely concerned with monsoon climate and alluvial lithology. Physical weathering becomes intensive due to the large temperature range along with 100 cm annual rainfall and is extensive as a result of the low relief. The annual temperature range of 5–40 °C has great significance in mechanical weathering due to the effective expansion and contraction phenomena. It also increases the reaction rate of chemical weathering up to 6–9 times. There is a tendency for doubling or tripling the rate of chemical weathering reaction for every 10 °C increase
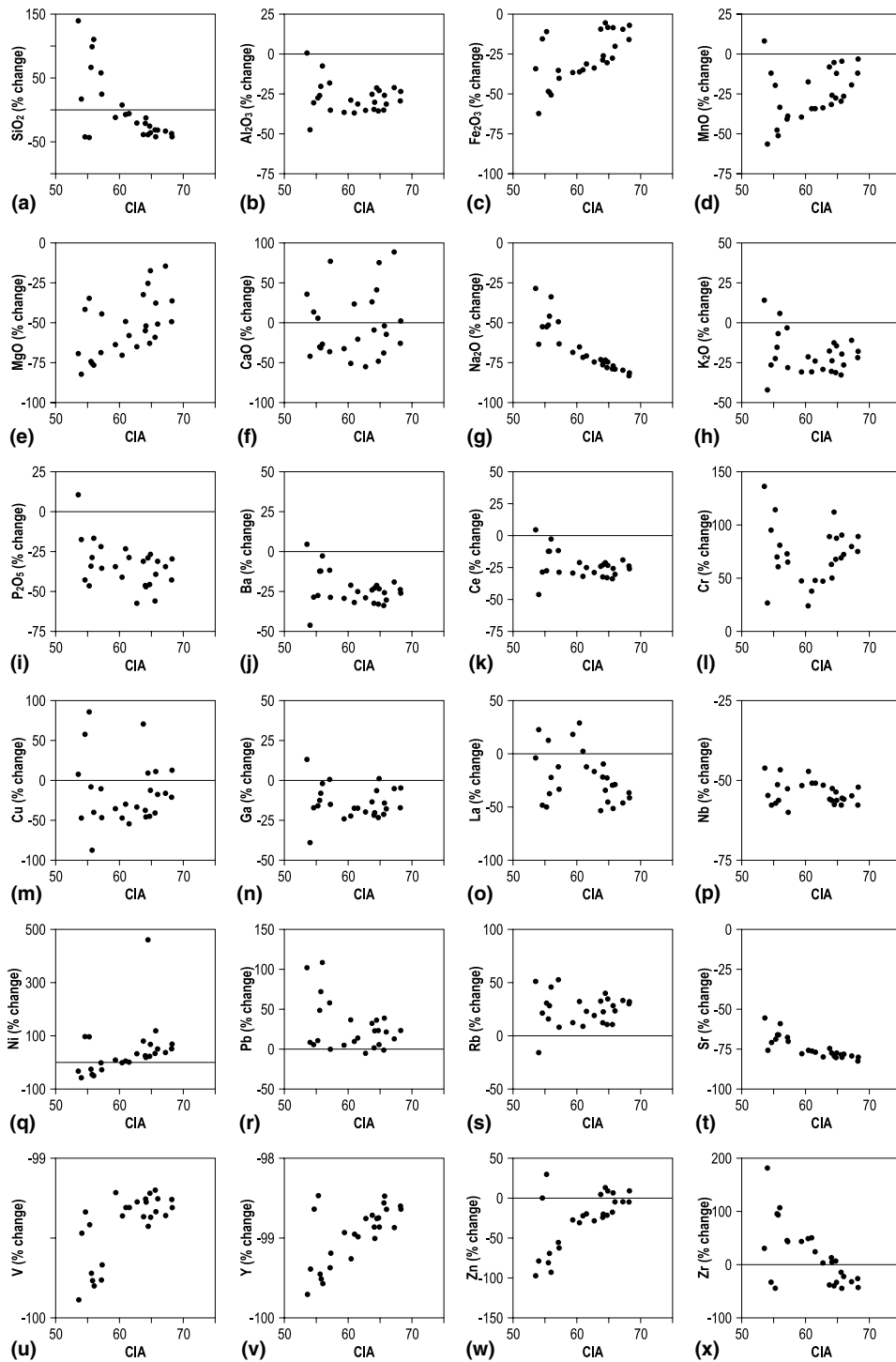
Fig. 14. Chemical mobility during the Ganga alluvial plain weathering processes. It is calculated in terms of percentage change (normalised with respect to TiO_2) of individual major/trace elements vs. progressive degree of chemical alteration (CIA values).

in temperature (Visher, 1945). Chemical weathering within the GAP proceeds to incipient and moderate stages. Weathering products, once formed, are removed

by the monsoon rains controlled fluvial process. The intensity and duration of monsoon precipitation are largely responsible for quantitative erosion of the GAP
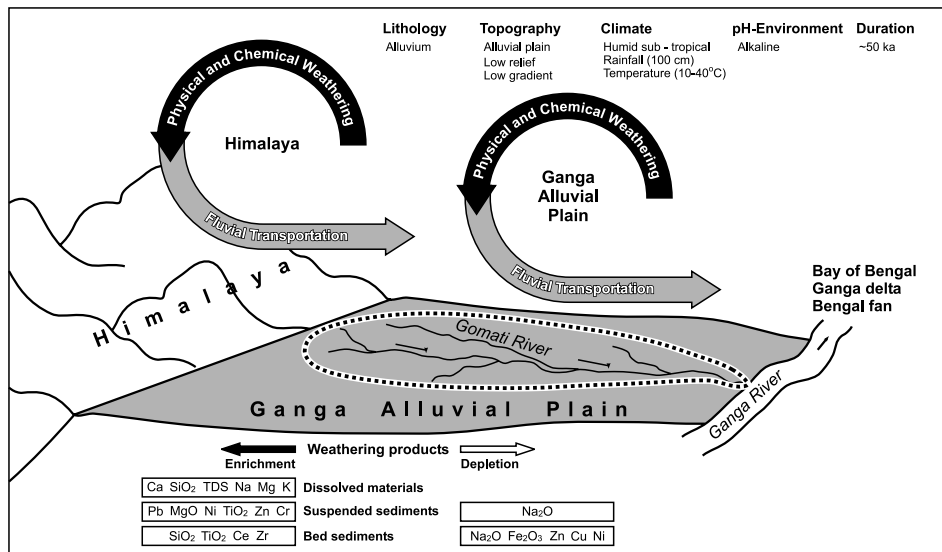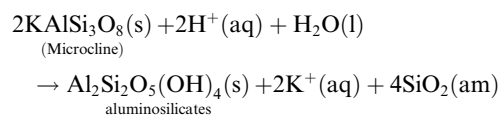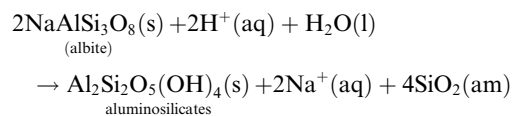
Fig. 15. Model representing the Ganga alluvial plain weathering processes and geochemical changes in its weathering products.

weathering products. In an extensive and low gradient fluvial system, time spent by sediments in temporary storage in alluvial sequences is also significant. During storage, chemical weathering has an extended time to operate and to remove labile constituents. Johnsson and Meade (1990) demonstrated that alluvial storage provides sufficient time for significant modification of sediment composition through chemical weathering in the tropical environments. In the GAP, advanced weathering does not proceed, as the weathering products do not accumulate to be themselves weathered.

Fig. 15 exhibits a complementary model of the GAP weathering processes. The Gomati River recycles the Himalayan derived sediments deposited in the Ganga Foreland Basin in Late Pleistocene–Holocene. The river also acts as a transporting agent to carry the weathering products originating by the GAP weathering process under humid sub-tropical climate. These weathering products have experienced "two cycle of weathering" before they get deposited in the depositional sites. The mineral content of the weathered material can be of great help in the study of the GAP weathering course. In the first cycle of weathering, illite is the dominant clay mineral ($\sim$80%) transported by rivers of the Himalayan region. In the second weathering cycle, smectite is the dominant clay mineral transported by several alluvial rivers of the GAP (Sarin et al., 1989). Rivers from the Himalaya add several cations and SiO_2 rich solutions to the GAP region, which is a possible build-up site for the synthesis of smectite type clay minerals formed by reaction of degraded aluminosilicates with dissolved SiO_2.

As weathering systems are open and irreversible, their chemical reactions are also irreversible because they take place as a result of disequilibrium between rocks and physico-chemical conditions. Following generalised weathering reactions that convert common minerals of alluvium to weathering products of the GAP. These weathering products demonstrate a progressive incomplete alteration of the alluvial sequence under the humid sub-tropical climate in last $\sim$50 ka of storage.

$$2NaAlSi_3O_8(s) + 2H^+(aq) + H_2O(l)$$
$$\text{(albite)}$$
$$\rightarrow Al_2Si_2O_5(OH)_4(s) + 2Na^+(aq) + 4SiO_2(am)$$
$$\text{aluminosilicates}$$

$$2KAlSi_3O_8(s) + 2H^+(aq) + H_2O(l)$$
$$\text{(Microcline)}$$
$$\rightarrow Al_2Si_2O_5(OH)_4(s) + 2K^+(aq) + 4SiO_2(am)$$
$$\text{aluminosilicates}$$

$$2K(Mg_2Fe)AlSi_3O_{10}(s) + 2H^+(aq) + H_2O(l)$$
$$\text{Biotite}$$
$$\rightarrow Al_2Si_2O_5(OH)_4(s) + 2Fe(OH)_3 + 2K^+(aq)$$
$$\text{Aluminosilicates}$$
$$+ 4Mg^+(aq) + 4SiO_2(am)$$

$$CaMg(CO_3)_2 + 4H^+(aq) \rightarrow Ca^{++}(aq) + Mg^{++}(aq)$$
$$\text{(Calcrete)}$$
$$+ 2H_2CO_3(aq)$$

$$7Al_2Si_2O_5(OH)_4 + Mg^{++}(aq) + 4SiO_2(am)$$
$$\text{aluminosilicates}$$
$$\rightarrow 6[Al_2Si_3O_{10}(OH)_2]Mg + 2H^+(aq) + 7H_2O(l)$$
$$\text{(Smectites)}$$

The above weathering reactions release a large array of bio-essential elements and, therefore, help to maintain

bio-productivity of the GAP. It is for this reason that the GAP is one of the highly fertile and densely-populated regions in the world.

6. Conclusions

The GAP exhibits a moderate degree of physical and chemical weathering of alluvium made up of the Himalayan derived sediments. It is evident that mineral sorting during fluvial transportation and deposition controls major and trace element distribution in the GAP weathering products. Major element geochemistry effectively characterizes the GAP weathering products as arkose to litharenite in rock classification. The GAP weathering products are transported into the Ganga River to the receiving and depositional sites: the Bay of Bengal, the Ganga Delta and the Bengal Fan. Sedimentary sequences of these depositional sites are made up of such weathering products. These depositional sedimentary sequences also preserve Quaternary climate change with glacial and inter-glacial events when temperatures were considerably lower and higher of the present day, respectively. Understanding the present day GAP weathering process can be useful for interpreting these sedimentary sequences of the Ganga Delta and the Bay of Bengal regions. It can also provide base level information for quantification of the geochemical cycling of the earth system that releases several cations for supporting life through nutrient supply. However, more detailed researches including hydrological investigation coupled with rare earth elements and isotopic geochemistry are required for an estimation of chemical and physical denudation of the GAP to quantify its contribution to causing the Ganga-Brahmaputra River System to be the world's largest sediment transporting system.

References

Abbas, N., Subramaniam, V., 1984. Erossion sediment transport in the Ganges river basin (India). J. Hydrol. 69, 173–182.

Ajmal, M., Khan, M.A., Nomani, A.A., 1985. Distribution of heavy metals in water and sediments of selected sites of Yamuna river (India). Environ. Monitor. Assess. 5, 205–214.

Ansari, A.A., Singh, I.B., Tobschall, H.J., 1998. Role of monsoon rains on concentrations and dispersion patterns of metal pollutants in sediments and soils of the Ganga Plain, India. Environ. Geol. 39, 221–237.

Ansari, A.A., Singh, I.B., Tobschall, H.J., 2001. Importance of geomorphology and sedimentation processes for metal dispersion in sediments and soils of the Ganga Plain: Identification of geochemical domains. Chem. Geol. 162, 245–266.

Berner, E.K., Berner, R.A., 1987. The Global Water Cycle. Prentice-Hall, Englewood Cliffs, NJ.

Berner, E.K., Berner, R.A., 1996. Global Environment: Water, Air and Geochemical Cycles. Prentice Hall, Inc, Upper Saddle River, NJ.

Bhatia, M.R., 1983. Plate tectonics and geochemical composition of sandstone. J. Geol. 91, 611–627.

Canfield, D.E., 1997. The geochemistry of river particulates from the continental USA: Major elements. Geochim. Cosmochim. Acta 61, 3349–3365.

Chakrapani, G.J., Subramanian, V., Gibbs, R.J., Jha, P.K., 1995. Size characteristics and mineralogy of suspended sediments of the Ganga River, India. Environ. Geol. 25, 192–196.

Chesworth, W., Dejou, J., Larroque, P., 1981. The weathering of basalts and relative mobilities of the major elements at Belbex, France. Geochim. Cosmochim. Acta 45, 1235–1243.

Cullers, R., 1988. Mineralogical and chemical changes of soil and stream sediment formed by intense weathering of Danburg granite, Georgia, USA. Lithos 21, 301–314.

Deer, W.A., Howie, R.A., Zussman, J., 1966. An Introduction to the Rock-Forming Minerals. Longman, England.

Drever, J.I., 1988. The Geochemistry of Natural Waters. Prentice-Hall, Englewood Cliff, NJ.

Dupré, B., Gaillardet, J., Rousseau, D., Allergre, C.J., 1996. Major and trace elements of river-borne material: The Congo Basin. Geochim. Cosmochim. Acta 60, 1301–1321.

Faruqui, N.H., Nagar, M., Dutta, A.K., 1992. Geoenvironmental apprisal of parts of Ganga Basin, Uttar Pradesh. In: Singh, I.B. (Ed.) Gangetic Plain: Terra Incognita. Geology Department, University of Lucknow, Lucknow, India, pp. 49–53.

Fedo, C.M., Eriksson, K.A., Krogstad, E.J., 1996. Geochemistry of shales from the Archen (~3.0 Ga) Buhwa Greenstone Belt, Zimbabwe: implications for provenance and

source-area weathering. Geochim. Cosmochim. Acta 60, 1751–1763.

Fritz, S.J., Mohr, D.W., 1984. Chemical alteration in the micro weathering environment with in a spheroidally weathered anorthite boulder. Geochim. Cosmochim. Acta 48, 2527–2535.

Galy, A., France-Lanord, C., 2001. Higher erosion rates in the Himalaya: Geochemical constrains on riverine fluxes. Geology 29, 23–26.

Garver, J.I., Scott, T.J., 1995. Trace elements in shale as indicators of crustal provenance and terrain accretion in southern Canadian Cordillera. Geol. Soc. Am. Bull. 107, 440–453.

Gupta, L.P., Subramanian, V., 1994. Environmental Geochemistry of the river Gomati: a tributary of the river Ganges. Environ. Geol. 24, 235–243.

Herron, M.M., 1988. Geochemical classification of terrigenous sands and shales from core or log data. J. Sed. Petrol. 58, 820–829.

Huh, Y., Tsoi, Mai-Yin, Zaitsev, A., Edmond, J.M., 1998. The fluvial geochemistry of the rivers of eastern Siberia: I. Tributaries of the Lena River draining the sedimentary platform of the Siberian Craton. Geochim. Cosmochim. Acta 62, 1657–1676.

Johnsson, M.J., Meade, R.H., 1990. Chemical weathering of fluvial sediments during alluvial storage: The Macuapanim Island point bar, Solimoes River. J. Sed. Petrol. 60, 827–842.

Kumar, S., 1989. Heavy metal pollution in Gomati River Sediments around Lucknow, Uttar Pradesh. Curr. Sci. 58, 557–559.

Kumar, S., Singh, I.B., 1978. Sedimentological study of Gomati river sediment, Uttar Pradesh, India: example of a river in alluvial plain. Senckenberg. Mar. 10, 145–221.

Loughnan, F.C., 1969. Chemical Weathering of Silicates Minerals. Elsevier, Amsterdam.

McLennan, S.M., 1995. Sediments and soils: chemistry and abundances. In: Ahrens, T.J. (Ed.), Rock Physics and Phase Relations: A Handbook of Physical Constants, vol. 3. American Geophysical Union Reference Shelf, pp. 8–19.

McLennan, S.M., Taylor, S.R., 1983. Geochemical evolution of the Archean shales from South Africa. I. The Swaziland and Pongola Supergroup: Precambrian Res. 22, 93–124.

McLennan, S.M., Nancy, W.B., Taylor, R., 1980. Rare earth element-thorium correlations in sedimentary rocks and the composition of the continental crust. Geochim. Cosmochim. Acta 44, 1833–1839.

Middelburg, J.J., Van Der Weijden, C.H., Woittiez, J.R.W., 1988. Chemical processes affecting the mobility of major, minor and trace elements during weathering of granite rocks. Chem. Geol. 68, 253–273.

Milliman, J.D., Meade, R.H., 1983. World-wide delivery of river sediment to the oceans. J. Geol. 91, 1–21.

Nagell, R.H., 1962. Geology of the Serro do Navio manganese district, Brazil. Econ. Geol. 57, 481–497.

Nesbitt, H.W., 1979. Mobility and fraction of rare earth elements during weathering of a granodiorite. Science 279, 206–210.

Nesbitt, H.W., Young, G.M., 1982. Early proterozoic climates and plate motions inferred from major element chemistry of lutites. Nature 299, 715–717.

Nesbitt, H.W., Young, G.M., 1984. Prediction of some weathering trends of plutonic and volcanic rocks based on thermodynamic and kinetic considerations. Geochim. Cosmochim. Acta 48, 1523–1534.

Nesbitt, H.W., Young, G.M., 1989. Formation and diagenesis of weathering profiles. J. Geol. 97, 129–147.

Nesbitt, H.W., Mackovics, G., Price, R.C., 1980. Chemical processes affecting alkalis and alkaline earth during continental weathering. Geochim. Cosmochim. Acta 44, 1659–1666.

Nesbitt, H.W., Young, G.M., Mclennan, S.M., Keays, R.R., 1996. Effects of chemical weathering and sorting on the petrogenesis of siliciclastic sediments, with implications for provenance studies. J. Geol. 104, 525–542.

Ollier, C., 1984. Weathering. Longman, New York.

Pettijohn, F.J., Potter, P.E., Siever, R., 1972. Sand and Sandstone. Springer, New York.

Potter, P.E., 1978. Petrology and chemistry of big river sands. J. Geol. 86, 423–449.

Potter, P.E., 1994. Modern sands of South America: composition, provenance and global significance. Geol. Rundschau. 83, 212–232.

Rao, K.L., 1975. India's Water Wealth. Orient Longman, New Delhi.

Rollinson, H.R., 1993. Using Geochemical Data: Evaluation Presentation, Interpretation. Longman, England.

Robinson, R.S., Johnsson, M.J., 1997. Chemical and physical weathering of fluvial sands in an artic environment: Sands of the Sagavanirktok River, North slope, Alaska. J. Sed. Petrol. 67, 560–570.

Sarin, M.M., Krishnaswami, S., Dilli, K., Somayajulu, B.L.K., Moore, W.S., 1989. Mojor ion chemistry of the Ganga–Brahmaputra river system: weathering processes and fluxes to the Bay of Bengal. Geochim. Cosmochim. Acta 58, 4809–4814.

Singh, I.B., 1996. Geological evolution of Ganga Plain – an overview. J. Palaeont. Soc. India 41, 99–137.

Singh, I.B., Srivastava, P., Sharma, S., Sharma, M., Singh, G., Rajgopalan, G., Shukla, U.K., 1999. Upland interfluve (Doab) deposition: alternative model to muddy overbank deposits. Facies 40, 197–210.

Singh, M., Ansari, A.A., Müller, G., Singh, I.B., 1997. Heavy metals in freshly deposited sediments of the Gomati River (a tributary of the Ganga river): Effects of human activities. Environ. Geol. 29, 246–252.

Singh, R.L., 1988. India: A Regional Geography. National Geographical Soc. India, Varanasi, India.

Srivastava, P., Singh, I.B., Sharma, M., Singhvi, A.K., 2003. Luminescnce chronology and late quaternary geomorphic history of the Ganga Plain, India. Palaeogeog. Palaeoclim. Palaeoecoe. 197, 15–41.

Stallard, R.F., 1988. Weathering and erosion in the Humid tropics. In: Lerman, A., Meybeck, M. (Eds.), Physical and Chemical Weathering in Geochemical Cycles. Kluwer, Dodretch, pp. 225–246.

Subramaniam, V., Sitasawad, R., Abbas, N., Jha, P.K., 1987a. Environmental Geology of the Ganga river basin. J. Geol. Soc. Ind. 30, 335–355.

Subramaniam, V., Van Grieken, R., Van't Dack, L., 1987b. Heavy metals distribution in the sediments of Ganges and Brahmaputra rivers. Environ. Geol. Water Sci. 9, 93–103.

Taylor, S.R., McLennan, S.M., 1981. The composition and evolution of the continental crust: rare earth element

evidence from sedimentary rocks. Philos. Trans. R. Soc. A 301, 381–399.

Taylor, S.R., McLennan, S.M., 1985. The Continental Crust: its Composition and Evolution. Oxford, Blackwells, London.

Visher, S.S., 1945. Climatic maps of geological interest. Bull. Geol. Soc. Am. 56, 713–736.

Vital, H., Stattegger, K., 2000. Major and trace elements of stream sediments from the lowermost Amazon River. Chem. Geol. 168, 151–168.

Wronkiewicz, D.J., Condie, K.C., 1987. Geochemistry of Archean shales from the Witwaterstrand Supergroup, South Africa: source area weathering and provenance. Geochim. Cosmochim. Acta 51, 2401–2416.